Available online at www.sciencedirect.com
SCIENCE DIRECT
Journal of Magnetic Resonance 179 (2006) 311–316
JMR Journal of Magnetic Resonance
www.elsevier.com/locate/jmr

Communication

Homogeneous broadenings in 2D solid-state NMR of half-integer quadrupolar nuclei

J.P. Amoureux *, J. Trébosc

UCCS, CNRS-8181, University of Lille-1, ENSCL Bâtiment C7, 59652 Villeneuve d'Ascq Cedex, France

Received 23 November 2005; revised 4 January 2006
Available online 3 February 2006

Abstract

The question of the homogeneous broadening that occurs in 2D solid-state NMR experiments is examined. This homogeneous broadening is mathematically introduced in a simple way, versus the irreversible decay rates related to the coherences that are involved during t_1 and t_2. We give the pulse sequences and coherence transfer pathways that are used to measure these decay rates. On $AlPO_4$ berlinite, we have measured the ^{27}Al echo-type relaxation times of the central and satellite transitions on 1Q levels, so that of coherences that are situated on 2Q, 3Q, and 5Q levels. We compare the broadenings that can be deduced from these relaxation times to those directly observed on the isotropic projection of berlinite with multiple-quantum magic-angle spinning (MAS), or satellite-transition MAS. We show that the choice of the high-resolution method, should be done according to the spin value and the corresponding homogeneous broadening.

Keywords: Magic-angle spinning NMR; Quadrupolar nuclei; Multiple-quantum MAS; Satellite-transition MAS; High-resolution; Homogeneous broadening

High resolution solid-state NMR of polycrystalline powders faces various anisotropic interactions [1] that have to be removed for high-resolution purposes. Until late 1980s, for nuclei with spin value $S > 1/2$, submitted to large electric quadrupole interactions, the second-order quadrupolar line broadening was the ultimate broadening not reduced by magic-angle spinning (MAS). MAS averages all first-order broadenings, but scales the central transition (CT: $1/2 \leftrightarrow -1/2$) linewidth of half-integer quadrupolar nuclei by a factor of only roughly three. A better resolution for such cases is obtained by more complex motions of the sample. Complete spatial averaging requires either mechanical rotation around two axes, as in double rotation (DOR) [2], or correlation of signals acquired at two different angles in a two-dimensional (2D) experiment as in dynamic angle spinning (DAS) [3]. However, both methods present many technical shortcomings. Frydman and Harwood [4] have demonstrated that line narrowing of the CT can be obtained without changing the orientation of the spinning axis. The 2D method thus derived, called multiple quantum MAS (MQMAS), correlates both second-order patterns of multiple quantum (MQ) and CT coherences and allows of extraction of isotropic information. More recently, a new class of 2D experiments, called Satellite Transition MAS (STMAS), has been introduced [5], which correlates second-order patterns of STs during t_1 with those of CT during t_2. The most recently proposed STMAS methods remove all unwanted signals by using a double-quantum filter (DQF), which is a CT-selective π pulse [6]. This pulse has been used in three different versions of STMAS: the DQF-STMAS and the double-quantum (DQ) STMAS experiments, which only differ by the fact the selective π pulse is at the end (DQF-STMAS) or at the beginning (DQ-STMAS) of the t_1 period [6], and the t_1-split STMAS for spin 3/2 nuclei [7]. In 1D experiments, the same filtration principle can also be used, simultaneously with a rotor-synchronized acquisition, to enhance by a factor 24/7 the resolution that can be observed

* Corresponding author. Fax: +33 3 20 43 68 14.
E-mail address: jean-paul.amoureux@univ-lille1.fr (J.P. Amoureux).

1090-7807/$ - see front matter © 2006 Elsevier Inc. All rights reserved.
doi:10.1016/j.jmr.2006.01.008

for spin $S = 5/2$ nuclei, leading to the DQF-SATRAS experiment [8]. The comparison of all MQMAS (3QMAS, 5QMAS [9], etc.) and STMAS (DQF, DQ, t_1-split, etc.) results has been facilitated recently by the introduction of a unified representation for all 2D methods [10]. In this representation, that we will use in the following, resonances are always located at the same places in the 2D spectra, which means that they always have the same isotropic (δ_{iso}) and anisotropic (δ_2) projections. However, differences in resolutions between the various techniques have been observed, but these differences remained poorly understood for several years. Recently, this issue has been addressed for the first time for MQMAS methods [11], and it has been shown that these differences of resolutions are mainly related to homogeneous irreversible decays that occur on the coherences that are involved from the excitation pulse until the refocusing of the second-order quadrupole interaction occurring at $t_{2e} = Rt_1$.

In this communication, we extend the theory to all MQ/ST-MAS 2D experiments in the frame of unified representation. Moreover, we propose sequences that allow quantifying these extra-broadenings. On a test sample, $AlPO_4$ berlinite, we have measured the ^{27}Al transverse spin–echo decay time constants of the CT and ST_1 ($\pm 3/2 \leftrightarrow \pm 1/2$) on 1Q levels, and of coherences that are situated on 2Q ($\pm 3/2 \leftrightarrow \mp 1/2$), 3Q ($\pm 3/2 \leftrightarrow \mp 3/2$), and 5Q ($\pm 5/2 \leftrightarrow \mp 5/2$) levels. We compare the broadenings that can be deduced from these relaxation times to those that are directly observed on the isotropic projection of berlinite with 3QMAS and 5QMAS, or with DQF-STMAS and DQ-STMAS.

In the following, we will only consider the echo pathway of 2D experiments, as the anti-echo signal is either not recorded, or only used to cancel the dispersive parts in amplitude-modulated experiments [12]. The coherence transfer pathway of the echo-signal of all MQ/ST-MAS amplitude-modulated experiments can always be described in the same way: $0Q \rightarrow pQ\ (t_1) \rightarrow -1Q\ (CT, t_2)$. Let us call T_{CT} and $T_p = \alpha T_{CT}$ the transverse homogeneous relaxation times of the CT ($-1Q$, t_2) and pQ (t_1) coherences, respectively. The 2D signal can be written:

$$s(t_1, t_2) = \exp\left(i(\omega_p t_1 + \omega_{CT} t_2) - \frac{t_1}{\alpha T_{CT}} - \frac{t_2}{T_{CT}}\right). \quad (1)$$

The isotropic signal corresponds to the top of the echo ($t_{2e} = Rt_1$, with $R > 0$), which means that all anisotropic terms disappear:

$$s(t_1, Rt_1) = \exp\left(\left\{ i(p-R)\cdot v_0 \left[\delta_{CS} + \frac{(\delta^p_{QIS} + R\delta^{CT}_{QIS})}{p-R}\right] - \frac{1}{\alpha T_{CT}} - \frac{R}{T_{CT}}\right\}\cdot t_1\right), \quad (2)$$

where v_0 is the Larmor frequency, and δ_{CS} and δ_{QIS} are the actual-chemical and quadrupolar-induced shifts, respectively. It has been shown that this equation can be simplified [10,13]:

$$s(t_1, Rt_1) = \exp\left(\left\{-iv_0^{app}\delta_{iso} - \frac{1}{T_{tot}}\right\}.t_1\right), \quad (3)$$

with

$$v_0^{app} = (R-p)v_0; \quad \delta_{iso} = \delta_{CS} - 10\delta^{CT}_{QIS}/17 + 10^6 m_I J/v_0;$$
$$T_{tot} = \alpha T_{CT}/(1+\alpha R). \quad (4)$$

The unified ppm scaling consists in using v_0^{app} instead of v_0 [10,13]. J is the scalar coupling constant between spin S and another spin I with magnetic number m_I. After Fourier and shearing transforms, isotropic projections are thus independent on the 2D high-resolution method, when unified ppm scaling is used, and when only inhomogeneous interactions are taken into account (Eq. (3), without the relaxation term) [10,13]. These interactions may be of different types, such as chemical and quadrupolar-induced shifts, scalar couplings, hetero-nuclear dipolar interactions, and quadrupolar-dipolar cross-terms [14]. In the case of distributed surroundings, such as amorphous samples, these interactions lead to broad resonances. This may be also the case of inhomogeneous static magnetic fields. One possible explanation for the variation of isotropic resolution in 3QMAS and 5QMAS experiments has been proposed, based on the difference of excitation versus the quadrupolar tensor orientation with respect to the RF-field [13]. However, this explanation does not apply when using strong RF-field amplitudes. Therefore, the only remaining explanation for the changes of isotropic resolutions, may thus arise from the homogeneous relaxation term [11]. This term leads, in unified ppm scaling, to a broadening (full-width at half-maximum: FWHM) equal to

$$B\ (\text{ppm}) = \frac{10^6 \cdot (1+\alpha R)}{\alpha\pi v_0 \cdot |R-p| \cdot T_{CT}}. \quad (5)$$

Most of the time, T_p and T_{CT} relaxation time values are close, and hence $\alpha \approx 1$. The broadenings described in Table 1 correspond to 3QMAS, 5QMAS, DQF-STMAS, and DQ-STMAS experiments, in the case of $\alpha = 1$.

It is important to note that homogeneous broadenings largely increase with the spin value. Indeed, they are multiplied by a factor of ca. 16, 7.5, and 20, in 3QMAS, DQF-STMAS, and DQ-STMAS, respectively, when increasing the spin value from 3/2 to 9/2 (Table 1).

In the case of all STMAS-based experiments, ST coherences are submitted to first-order quadrupole interactions during t_1. When the nuclei undergo molecular motions with a frequency approximately equal to the quadrupole interaction, the homogeneous transverse relaxation times of the ST coherences decrease largely [15]. This is not the case for the CT and MQ coherences involved in MQMAS, which are only submitted to second-order quadrupole interactions. In STMAS-based experiments, these motions result in a large decrease of the α ratio, and hence to a large increase of the broadening, especially for high-spin value, leading to the disappearing of the signal:

Table 1
Broadening (B) in unified ppm scaling, given in $10^6/\pi\nu_0 T_{CT}$ unit, calculated with $\alpha = 1$ in Eq. (5)

S	3Q B	3Q $1/\lvert R-p\rvert$	5Q B	5Q $1/\lvert R-p\rvert$	DQF-ST B	DQ-ST B	DQF/DQ $1/\lvert R-p\rvert$
3/2	8/17	9/34			17/17	10/17	9/17
5/2	31/17	24/34	37/85	12/85	31/17	55/17	24/17
7/2	73/17	45/34	50/85	22.5/85	73/17	118/17	45/17
9/2	127/17	72/34	131/85	36/85	127/17	199/17	72/17

$1/\lvert R-p\rvert$ defines the indirect spectral-width, $\Delta\delta_{iso} = \frac{\nu_R}{\nu_0 \cdot \lvert R-p\rvert}$, after shearing of rotor-synchronized experiments.

$$B\ (\text{ppm}) \approx \frac{10^6}{\alpha\pi\nu_0 \cdot |R-p| \cdot T_{CT}}. \quad (6)$$

In Fig. 1, we show the sequences and pathways that allow measuring the homogeneous relaxation times of all coherences involved in MQMAS (a), and STMAS (b) methods. These experiments are very easy to setup since all pulses are the same as for MQMAS or STMAS, except the extra middle hard-pulse length that must be optimized to get maximum signal. These sequences are relatively efficient, leading to spectrometer times of only a few hours; except for the measurements of T_{5Q}, which requires an additional jump of 10 quanta levels with respect to the classical 5QMAS experiment which is by itself not a very efficient method.

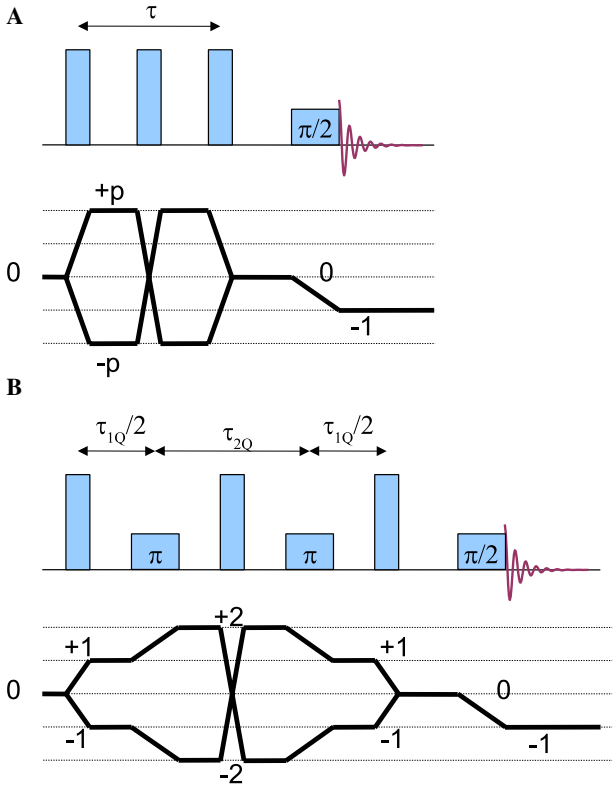

Fig. 1. Pulse sequences and coherence transfer pathways to measure. (A) T_{CT}, T_{3Q}, T_{5Q} ($p = 1$, 3, and 5, respectively), and (B) ($T_{ST,1Q}$) or ($T_{ST,2Q}$). In (A) the three pulses are either CT selective ($\pi/2$, π, and $\pi/2$) pulses for T_{CT}, or strong hard-pulses for T_{3Q} and T_{5Q}. In (B) the two selective π pulse are close either to the central hard-pulse ($\tau_{2Q} = 0$, $T_{ST,1Q}$) or to the two external hard-pulses ($\tau_{1Q} = 0$, $T_{ST,2Q}$).

As a test sample, we have chosen ^{27}Al NMR of $AlPO_4$ berlinite, which contains a single aluminum species with quadrupolar parameters: $C_Q = 4.07$ MHz and $\eta_Q = 0.34$. It must be reminded that the rotation axis must be perfectly adjusted at the magic-angle in STMAS-based experiments, but that this is not mandatory for MQMAS experiments, and it has even been shown that T_p can be increased by spinning slightly off-magic angle [16]. We have observed such a behavior for T_{CT}, T_{3Q}, and T_{5Q} of berlinite, and this allowed to increase these values by a factor of 1.3–1.8 with respect to their values at the magic angle. All spectra were recorded at 9.4 T, with a 3.2-mm rotor using $\nu_R = 20$ kHz and RF-fields of 160 and 5 kHz for the hard and soft pulses, respectively. Two homogeneous attenuation curves are displayed, versus the delay τ, in Fig. 2. The accuracy of the measurements was good, except for 5QMAS were the S/N ratio was poor in spite of a 4 day accumulation (Fig. 2). The experimental results are given in Table 2.

The experimental off magic-angle ratio $T_{5Q}/T_{3Q} = 1.2$ is slightly smaller than the factor 1.4, as calculated with the Redfield relaxation theory in the slow motional limit [11]. The isotropic homogeneous broadenings calculated using Eq. (5), are not very different in MQMAS from those obtained (Table 1) by assuming all relaxation times equal to T_{CT} (Table 3). In STMAS, this approximation is not as

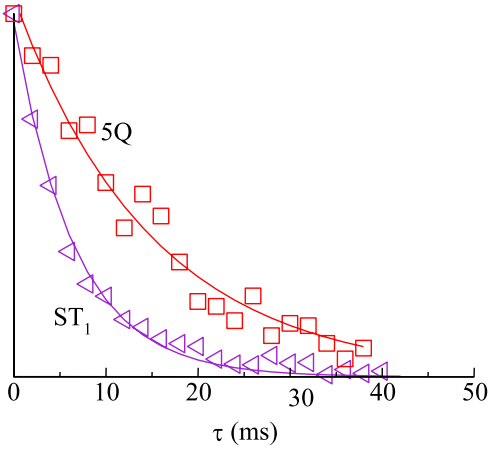

Fig. 2. Homogeneous attenuation curves versus τ (equal to $\tau_{1Q} + \tau_{2Q}$ for ST_1) to measure either on magic-angle $T_{ST,1Q} = 6.5$ ms (◁), or slightly off magic-angle $T_{5Q} = 15$ ms (□) values. Continuous curves represent the fit of the experimental data. Those corresponding to T_{5Q} show the relative inaccuracy of the results. For all other measurements, the accuracy was as good as for $T_{ST,1Q}$.

Table 2
Irreversible decay rates (ms) corresponding to the various coherences

	T_{CT}	T_{3Q}	T_{5Q}	$T_{ST,1Q}$	$T_{ST,2Q}$
On magic-angle	10 ± 0.5	7 ± 0.5		6.5 ± 0.5	6 ± 0.5
Off magic-angle	13 ± 0.5	12.5 ± 0.5	15 ± 1.5		

These decay rates allow us to calculate the α values, which are involved in Table 3.

good as for MQMAS, because the difference between T_{ST} and T_{CT} values is amplified by the R and p parameters in Eq. (5). In Fig. 3A, we show the isotropic sheared projections of berlinite, and in Table 3 we give their experimental linewidths (B_{exp}). As previously said, there are two experimental parameters that may change the isotropic projections: the position of the rotation axis, which changes the T_{3Q} and T_{5Q} values in MQMAS [16] and introduces a small first-order quadrupolar contribution in STMAS [5], so as the spinning speed fluctuations in STMAS [17]. For this reason, the direct comparison of homogeneous broadenings can only be made in between 3QMAS and 5QMAS or DQF-STMAS and DQ-STMAS. As expected, the on magic-angle 3QMAS experimental resolution is broader (by 0.28 ppm) than that observed off magic-angle (Table 3). One can observe a difference of $\Delta B_{exp} = 0.32$ ppm between the 3Q- and 5QMAS experimental off magic-angle isotropic linewidths, which is in agreement with the previous values deduced from the measured T_2' values: $\Delta B_{calc}^{hom} = 0.34$ ppm. By using Eq. (5), it is possible to deduce from the 5QMAS isotropic spectrum (better resolution than 3QMAS), the true inhomogeneous MQMAS linewidth of berlinite, which is thus equal to ca. $B_{MQ}^{inh} = 0.60$ ppm (0.70–0.10). The difference between DQ- and DQF-STMAS experimental linewidths ($\Delta B_{exp} = 0.45$ ppm), is also in agreement with values deduced from Eq. (5) ($\Delta B_{calc}^{hom} = 0.49$ ppm). However, the inhomogeneous STMAS linewidths ($B_{ST}^{inh} = B_{exp} - B_{calc}^{hom} = 0.91$ ppm (DQF) or 0.87 ppm (DQ)) are broader than the inhomogeneous MQMAS linewidth ($B_{MQ}^{inh} = 0.60$ ppm). The extra inhomogeneous broadening, which is identical for both STMAS experiments, is related to experimental imperfections (magic angle mis-setting and spinning speed fluctuations). Its value, can be evaluated with Eq. (5), from the experimental DQF-STMAS isotropic projection (better resolution than DQ-STMAS), to 0.31 ppm (FWHM) (1.70–0.60–0.79), which means a total (FW at 0%) extra-broadening of ca. 0.8 ppm. It has been

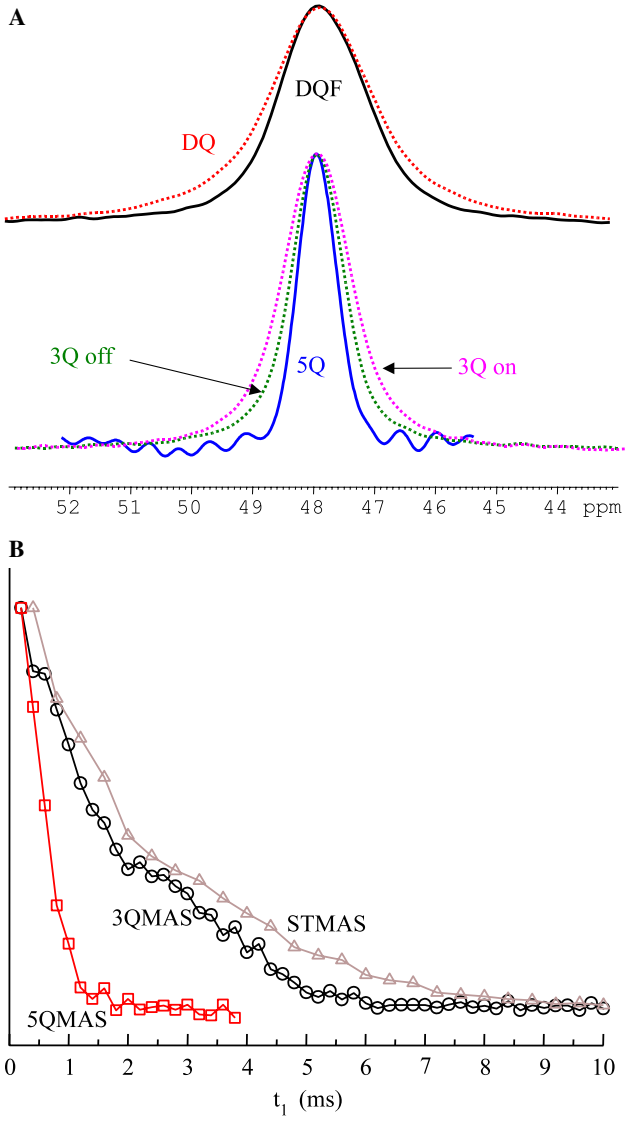

Fig. 3. (A) Isotropic sheared projections in unified ppm scaling of either DQ-STMAS and DQF-STMAS on top, or *on* magic-angle 3QMAS and *off* magic-angle 3QMAS and 5QMAS on bottom. (B) Fids versus t_1, corresponding to $\int s(t_1, v_2) \cdot dv_2$, for STMAS (DQ or DQF) (△) and off magic-angle 3QMAS (○), and 5QMAS (□).

shown that the total isotropic linewidth in STMAS-based experiments related to ill-setting of the magic-angle is equal to $\Delta\delta_{iso}$ (ppm) $\approx 10453 C_Q \Delta\theta / \nu_0$, for spin 5/2 nuclei [18]. By neglecting the spinning speed fluctuations, we can thus calculate the off magic-angle setting to be $\Delta\theta < 0.002°$.

Table 3
Broadenings (FWHM) expressed in unified ppm scaling; *off* or *on* magic-angle

	3QMAS *on*	3QMAS *off*	5QMAS *off*	DQF-STMAS *on*	DQ-STMAS *on*
B_{exp}	1.30	1.02	0.70	1.70	2.15
B_{calc}^{hom}	0.65	0.44	0.10	0.79	1.28
$B_{calc}^{hom}(\alpha = 1)$	0.55	0.43	0.09	0.56	1.00
$B^{inh} = B_{exp} - B_{calc}^{hom}$	0.65	0.58	0.60	0.91	0.87

Let us analyze first the results we have obtained for 2D experiments. By looking to Eq. (3), it can be shown that if inhomogeneous broadening dominates the linewidth, the evolution time required to not truncate the signal in the indirect dimension is inverse proportional to ν_0^{app} and hence to $|R-p|$. On the contrary, if homogeneous broadening contributes most, evolution time is proportional to T_{tot}. Fig. 3B shows the time evolution, versus t_1, of the signal integrated over ν_2 : $\int s(t_1,\nu_2)\cdot \mathrm{d}\nu_2$. The 3QMAS decay time is ca. five times larger than that of 5QMAS. This factor corresponds to the $|R-p|_{5Q}/|R-p|_{3Q}$ ratio, and is much larger than the ratio $T_{\text{tot, 3Q}}/T_{\text{tot, 5Q}} = 1.1$ due to homogeneous contributions. It is important to remark, that the contribution of the homogeneous interactions is often small onto the evolution of the signal in the indirect dimension, but can be larger than that due to inhomogeneous interactions on the isotropic linewidth in case of well-crystallized compounds: $B^{\text{hom}}_{\text{3Q,ON}} = 0.65$ ppm and $B^{\text{inh}} = 0.60$ ppm in berlinite. From the $|R-p|$ factors (Table 1), the signal decay of DQ- and DQF-STMAS signals should be twice slower than that of 3QMAS. The decay times of these two experiments are indeed identical, but are only ca. 25% larger than that of 3QMAS. This too fast decay, with respect to the inhomogeneous contributions, observed in the indirect dimension of STMAS, is related to the same experimental imperfections which introduced an extra isotropic broadening in Fig. 3A: ill magic-angle setting and spinning speed fluctuations.

Because only second-order dephasings are refocused by STMAS sequences, it is mandatory to then always rotor-synchronize the evolution time t_1. In MQMAS it is highly recommended to do the same for three reasons: (i) a small number of t_1 steps are then used, thereby minimizing the acquisition time, (ii) all sidebands are aliased onto the center band, thus maximizing the S/N ratio and simplifying the interpretation of the spectra, and (iii) distortions with respect to MAS spectra are minimized [19]. It can be shown, and verified in case of berlinite (spectra not shown), that in case of rotor-synchronized 2D experiments, the indirect sheared spectral width is equal to $\Delta\delta_{\text{iso}} = \frac{\nu_R}{\nu_0\cdot|R-p|}$. In rotor-synchronized conditions, the indirect decay rate (Fig. 3B) gives the number of t_1 steps required to not truncate the signal.

It must be noted that results previously described for MQ/ST-MAS amplitude-modulated sequences, also apply to full-echo MQMAS [20], full-echo STMAS [21] or MQ/ST-DOR experiments [22].

The two STMAS-based experiments (DQF, DQ) have the same efficiency concerning their coherence transfer pathways, the same indirect spectral width and the same minimum number of rotor-synchronized t_1 steps (same $|R-p|$ factor). Moreover, they present the same sensitivity to spinning-speed fluctuations and off magic-angle setting. The choice of the STMAS method should thus be done according to the behavior of the sequences to the homogeneous broadening, especially for large spin values where it becomes very important.

5QMAS experiments are much less sensitive to homogeneous broadenings than 3QMAS (Table 1), and thus will display a better resolution, especially with large spin value, if homogeneous interactions are not weak. However, 5QMAS presents two main limitations: its limited indirect spectral width and its poor efficiency. Indeed, its rotor-synchronized spectral width is five times smaller than with 3QMAS, and it may be insufficient in case of large chemical shift spread or Larmor frequency and/or slow spinning speed. In this case the t_1 step can be fixed to a sub-multiple of the rotor period with the drawback of several spinning sidebands along the indirect dimension. To compare the experimental times required by rotor-synchronized 3QMAS and 5QMAS experiments, three different types of parameters must be taken into account: the linewidth on MQ levels, the number of rotor-synchronized t_1 steps, and the efficiency of the coherence transfer pathways. As the two first parameters are inverse proportional of each other, the S/N ratio per unit time is only related to the third one: the efficiencies of the transfers. Typically, 5Q transfers are approximately 5 times less efficient than 3Q transfers [23]. Therefore, an experiment lasting ca. 25 times longer in 5QMAS than in 3QMAS is expected to obtain the same S/N ratio.

Previous calculation can easily be extended to t_1-split [7] and split-t_1 [24] methods, in which the evolution time t_1 is split into two periods where the magnetization evolves on two complementary coherences chosen in such a way that the refocusing always occurs at $t_2 = 0$.

In all 1D experiments, the homogeneous broadening is equal to $10^6/\pi T\nu_0$, where T is the homogeneous relaxation decay of the observed coherence: CT in MAS and DOR [2], or inner-STs in DQF-SATRAS [8]. This means that for spins 5/2, 7/2, and 9/2, the homogeneous broadening observed in 3QMAS and all STMAS-based 2D experiments will always be larger than with MAS, DOR, and DQF-SATRAS (if $T_{\text{STi}} \approx T_{\text{CT}}$) 1D experiments. It must be noted that in DAS, the broadening is always equal to $10^6/\pi\nu_0 T_{\text{CT}}$.

In conclusion, homogeneous isotropic broadenings observed in quadrupolar high-resolution 2D methods, can be easily explained and quantified with simple high-resolution echo-type experiments. This broadening effect increases largely with the spin value. These results permit to choose the experiment minimizing the effect of homogeneous broadening. In the MQMAS case, we have shown how, at the expense of sensitivity, 5QMAS can dramatically increase the resolution if the linewidth stems from homogeneous interactions. In the STMAS case, only homogeneous broadenings are involved in resolution difference between DQF-STMAS and DQ-STMAS methods. Thus, DQ-STMAS should achieve a better resolution than DQF-STMAS for spins 3/2 and DQF-STMAS should be used for spins greater or equal to 5/2. We have proposed pulse sequences to quantify these effects. Phase-cycling corresponding to these sequences can be downloaded from: http://univ-lille1/lcps/pulse_nmr.

Acknowledgments

Authors thank Region Nord/Pas de Calais, Europe (FEDER), CNRS, French Minister of Science, USTL, ENSCL, and the Bruker and Cortec companies for funding.

References

[1] A. Abragam, Principles of Nuclear Magnetism, Oxford University Press, London, 1961.
[2] A. Samoson, E. Lipmaa, A. Pines, High-resolution solid-state NMR, averaging of second-order effect by means of a double-rotor, Mol. Phys. 65 (1988) 1013–1018.
[3] K.T. Mueller, B.Q. Sun, G.C. Chingas, J.W. Zwanziger, T. Terao, A. Pines, Dynamic-angle spinning of quadrupolar nuclei, J. Magn. Reson. 86 (1990) 470–487.
[4] L. Frydman, J.S. Harwood, Isotropic spectra of half-integer quadrupolar spins from bidimensional magic-angle-spinning NMR, J. Am. Chem. Soc. 117 (1995) 5367–5368.
[5] Z.H. Gan, Isotropic NMR spectra of half-integer quadrupolar nuclei using satellite transitions and magic-angle-spinning, J. Am. Chem. Soc. 122 (2000) 3242–3243.
[6] H.T. Kwak, Z.H. Gan, Double-quantum filtered STMAS, J. Magn. Reson. 164 (2003) 369–372.
[7] J.P. Amoureux, J. Trébosc, L. Delevoye, G. Fink, F. Taulelle, A. Flambard, L. Montagne, G. Tricot, M. Pruski, J. Wiench, S. Steuernagel, J. Frye, New Very Sensitive High-resolution NMR method for Quadrupolar Nuclei based on the SPAM Concept. 47th Rocky Mountain Conference, July 31st–August 4th, 2005, Denver, USA.
[8] S.E. Ashbrook, S. Wimperis, Rotor-synchronized acquisition of quadrupolar satellite-transition NMR spectra: practical aspects and double-quantum filtration, J. Magn. Reson. 177 (2005) 36–47.
[9] C. Fernandez, J.P. Amoureux, 2D multiple-quantum MAS NMR spectroscopy of ^{27}Al in alumino-phosphate molecular sieves, Chem. Phys. Lett. 242 (1995) 449–454.
[10] J.P. Amoureux, C. Huguenard, F. Engelke, F. Taulelle, Unified representation of MQMAS and STMAS NMR of half-integer quadrupolar nuclei, Chem. Phys. Lett. 356 (2002) 497–504.
[11] K.J. Pike, R.P. Malde, S.E. Ashbrook, J.Mc. Manus, S. Wimperis, Multiple-quantum MAS NMR of quadrupolar nuclei. Do five-, seven- and nine-quantum experiments yield higher resolution than the three-quantum experiment? Solid State. NMR 16 (2000) 203–215.
[12] J.P. Amoureux, C. Fernandez, S. Steuernagel, Z-filtering in MQMAS NMR, J. Magn. Reson. A123 (1996) 116–118.
[13] J.P. Amoureux, C. Fernandez, Triple, quintuple and higher-order multiple quantum MAS NMR of quadrupolar nuclei, Solid State NMR 10 (1998) 211–223;
Solid State NMR 16 (2000) 339–343.
[14] J.Mc. Manus, R. Kemp-Harper, S. Wimperis, Second-order quadrupolar-dipolar broadening in two-dimensional multiple-quantum MAS NMR, Chem. Phys. Lett. 311 (1999) 292–298.
[15] S.E. Ashbrook, S. Antonijevic, A.J. Berry, S. Wimperis, Motional broadening: an important distinction between multiple-quantum and satellite-transition MAS NMR of quadrupolar nuclei, Chem. Phys. Lett. 364 (2002) 634–642.
[16] H.T. Kwak, P. Srinivasan, J. Quine, D. Massiot, Z. Gan, Satellite transition rotational resonance of homonuclear quadrupolar spins: magic-angle effect on spin–echo decay and inversion recovery, Chem. Phys. Lett. 376 (2003) 75–82.
[17] C. Huguenard, F. Taulelle, Z. Gan, Optimizing STMAS, J. Magn. Reson. 156 (2005) 131–137.
[18] J.P. Amoureux, L. Delevoye, G. Fink, F. Taulelle, A. Flambard, L. Montagne, Implementing SPAM into STMAS: a net sensitivity improvement in high-resolution NMR of quadrupolar nuclei, J. Magn. Reson. 175 (2005) 285–299.
[19] D. Massiot, Sensitivity and line shape improvements of MQMAS by rotor-synchronization, J. Magn. Reson. A122 (1996) 240–244.
[20] D. Massiot, B. Touzo, D. Trumeau, J.P. Coutures, J. Virlet, P. Florian, P.J. Grandinetti, Two-dimensional magic-angle spinning isoropic reconstruction sequences for quadrupolar nuclei, Solid State NMR 6 (1996) 73–83.
[21] K.J. Pike, S.E. Ashbrook, S. Wimperis, Two-dimensional STMAS NMR of quadrupolar nuclei: shifted echoes, high-spin nuclei and resolution, Chem. Phys. Lett. 345 (2001) 400–408.
[22] A. Samoson, Two-dimensional isotropic NMR of quadrupole nuclei in solids, J. Magn. Reson. A121 (1996) 209–211.
[23] C. Fernandez, J.P. Amoureux, J.M. Chezeau, L. Delmotte, H. Kessler, ^{27}Al MAS NMR characterization of $AlPO_4$-14 enhanced resolution and information by MQMAS, Microporous Mater. 6 (1996) 331–340.
[24] S.P. Brown, S. Wimperis, Two-dimensional MQMAS NMR of quadrupolar nuclei: a comparison of methods, J. Magn. Reson. 128 (1997) 42–61.